Involvement of the GTP Binding Protein Rho in Constitutive Endocytosis in *Xenopus laevis* Oocytes

Günther Schmalzing,* Hans-Peter Richter,‡ Alexander Hansen,‡§ Wolfgang Schwarz,* Ingo Just,§ and Klaus Aktories§

*Max-Planck-Institut für Biophysik, D-60528 Frankfurt, Germany; ‡Institut für Physiologie, Universität des Saarlandes, D-66421 Homburg-Saar, and §Institut für Pharmakologie und Toxikologie, Universität Freiburg, D-79109 Freiburg, Germany

Abstract. To study an endocytotic role of the GTP-binding protein RhoA in *Xenopus* oocytes, we have monitored changes in the surface expression of sodium pumps, the surface area of the oocyte and the uptake of the fluid-phase marker inulin. *Xenopus* oocytes possess intracellular sodium pumps that are continuously exchanged for surface sodium pumps by constitutive endo- and exocytosis. Injection of *Clostridium botulinum* C3 exoenzyme, which inactivates Rho by ADP-ribosylation, induced a redistribution of virtually all intracellular sodium pumps to the plasma membrane and increased the surface area of the oocytes. The identical effects were caused by injection of ADP-ribosylated recombinant RhoA into oocytes. The C3 exoenzyme acts by blocking constitutive endocytosis in oocytes, as determined using a mAb to the β1 subunit of the mouse sodium pump as a reporter molecule and oocytes expressing heterologous sodium pumps. In contrast, an increase in endocytosis and a decrease in the surface area was induced by injection of recombinant Val14-RhoA protein or Val14-*rhoA* cRNA. PMA stimulated sodium pump endocytosis, an effect that was blocked by a specific inhibitor of protein kinase C (Gö 16) or by ADP-ribosylation of Rho by C3. Similarly, the phorbol ester-induced increase in fluid-phase endocytosis in oocytes was inhibited by Gö 16, C3 transferase, or by injection of ADP-ribosylated RhoA. In contrast to C3 transferase, *C. botulinum* C2 transferase, which ADP-ribosylates actin, had no effect on sodium pump endocytosis or PMA-stimulated fluid-phase endocytosis. The data suggests that RhoA is an essential component of a presumably clathrin-independent endocytic pathway in *Xenopus* oocytes which can be regulated by protein kinase C.

THERE is substantial evidence that GTP-binding proteins of the Ras superfamily play essential roles at virtually every stage of intracellular membrane transport (for recent reviews, see Gruenberg and Clague, 1992; Pfeffer, 1992; Ferro-Novick and Novick, 1993; Novick and Brennwald, 1993). Protein transport from the Golgi apparatus to the plasma membrane requires the expression of the Sec4 gene, which encodes a protein with 30% homology to Ras (Salminen and Novick, 1987). A similar yeast protein, Ypt1, has a role in ER to Golgi transport (Schmitt et al., 1988; Segev et al., 1988). Mammalian counterparts of Sec4 and Ypt1 have been grouped into a family denoted Rab proteins (Touchot et al., 1987; Haubruck et al., 1987) and also found to be essential for membrane traffic (for reviews, see Pfeffer, 1992; Ferro-Novick and Novick, 1993; Fischer v. Mollard et al., 1994). Owing to their variety and organelle-specific distribution (Chavrier et al., 1990), the different Rab proteins have been proposed to confer specificity to individual membrane targeting and/or fusion events (Rothman and Orci, 1992). Rab4 (van der Sluijs et al., 1992) and Rab5 (Bucci et al., 1992; Novick and Brennwald, 1993; Trowbridge et al., 1993) are, for instance, associated with the plasma membrane and early endosomes and involved in endocytosis; while Rab3a, which is predominantly found on synaptic vesicles, is involved in regulated exocytosis (Fischer v. Mollard et al., 1990, 1991).

In addition to Rab proteins, the ARF[1] and SAR families of Ras-like GTP binding proteins function in intracellular transport. ARF, characterized originally as ADP-ribosylating factor, is required for the assembly of the non-clathrin coatomer complex onto Golgi membranes (Donaldson et al., 1992; Palmer et al., 1993) and subsequent budding of COP-coated vesicles (Orci et al., 1993). It is also required for the membrane binding of the AP-1 adaptor particle, a clathrin coat protein (Stamnes and Rothman, 1993). Reconstitution and inhibition studies have revealed that ARF plays a role in several membrane trafficking events including intra-Golgi transport (Kahn et al., 1992), early

Address correspondence to Günther Schmalzing, Biocenter N260, Dept. of Pharmacology, Marie-Curie-Str. 9, D-60439 Frankfurt. Tel.: 49 69 798 29365. Fax: 49 69 798 29374. E-mail: Schmalzing@em.uni-frankfurt.de.

1. *Abbreviations used in this paper*: ARF, ADP-ribosylating factor; BSP, brain-specific protein; GST; glutathione-S-transferase; ORI, oocyte Ringer solution; PKC, protein kinase C.

endosome fusion (Lenhard et al., 1992), and nuclear membrane fusion in *Xenopus* egg extracts (Boman et al., 1992). SAR proteins are required for budding of transport vesicles from the ER (similar to Ypt1), but constitute a separate subfamily of Ras-related proteins. Like all GTP-binding proteins, the Ras-related proteins act as molecular switches, with an active GTP-bound form and an inactive GDP-bound form. Although the precise step-by-step function of Ras-like proteins in membrane traffic is unclear, most data supports the view that the GTP/GDP-induced conformational switching is paralleled by a membrane association-dissociation cycle.

The three mammalian Rho proteins (A, B, and C) and the two Rac proteins (1 and 2) are members of a separate subfamily of Ras-like proteins (Madaule and Axel, 1985; Didsbury et al., 1989) and are thought to be involved in the organization of the cytoskeleton. The C3 exoenzyme from *Clostridium botulinum* (Aktories et al., 1987; Braun et al., 1989) selectively ADP-ribosylates Rho proteins on asparagine 41 in the putative effector region (Sekine et al., 1989) and renders them biologically inactive (Paterson et al., 1990). Introduction of C3 into a variety of cells has been shown to alter the shape of these cells as a result of disassembly of actin microfilaments (Chardin et al., 1989; Paterson et al., 1990; Wiegers et al., 1991). Likewise, injection of Rho GDP dissociation inhibitor, which stabilizes the GDP-bound inactive form of Rho, mimics the C3 effect and induces rounding up of fibroblasts and the disappearance of actin stress fibers (Miura et al., 1993). When normal and mutant RhoA were microinjected into serum-starved fibroblasts, there was a rapid formation of actin stress fibers and focal adhesions (Ridley and Hall, 1992). This response, which was also observed after the external addition of serum, lysophosphatic acid, or bombesin, was blocked by the C3 exoenzyme (Ridley and Hall, 1992).

Rac proteins, sharing 60% identity with Rho (Didsbury et al., 1989), are required for superoxide generation by NADPH oxidase in phagocytic cells (Abo et al., 1991; Knaus et al., 1991). They are also involved in the organization of the actin cytoskeleton (Ridley et al., 1992). Microinjection of Rac1 or addition of growth factors stimulated actin filament accumulation at the plasma membrane to form membrane ruffles in confluent fibroblasts, while a pinocytotic accumulation of large vesicles was observed in subconfluent fibroblasts (Ridley et al., 1992). Rac1 activated Rho to stimulate the Rho-dependent formation of actin stress fibers (Ridley and Hall, 1992), an effect that was blocked by C3. Rac proteins have been reported to also be substrates of C3 in vitro (Didsbury et al., 1989). However, C3 failed to impair Rac1-induced membrane ruffling (Ridley and Hall, 1992), which is consistent with the low efficiency of C3-induced ADP-ribosylation of Rac in vivo (Just et al., 1992).

We have previously observed that exposure of prophase-arrested *Xenopus* oocytes to the tumor promoter PMA induces a pronounced reorganization of the plasma membrane, associated with a disappearance of virtually all microvilli (Vasilets et al., 1990) and the appearance of large pinocytotic vesicles underneath the cell surface (Schmalzing et al., 1991*b*). In these studies, changes in the surface expression of sodium pumps was shown to closely parallel changes in the surface area of the oocytes, suggesting that sodium pumps can serve as a general marker of cell surface recycling in these cells. Since fluid-phase endocytosis and membrane ruffling appear to be closely associated processes in various cells (Bar-Sagi et al., 1987; Keller, 1990), we considered the possibility that members of the Rho/Rac family are involved in the regulation of membrane organization of *Xenopus* oocytes. Here we report that Rho but not Rac proteins participate in the control of constitutive endocytosis in *Xenopus* oocytes. Furthermore, we present evidence that PMA acts through Rho to stimulate fluid-phase endocytosis.

Materials and Methods

Materials

C. botulinum C3 exoenzyme (Aktories et al., 1987, 1988), *Clostridium limosum* exoenzyme (Just et al., 1992), and *C. botulinum* C2 toxin (Ohishi et al., 1980) were purified as described. For microinjection, *botulinum* C3 exoenzyme and *limosum* exoenzyme were dissolved in 100 mM NaCl and 100 mM Na-phosphate, pH 7.5; C2 was dissolved in 50 mM triethanolamine-HCl, pH 7.5. PMA was obtained from Sigma Chem. Co. (Munich, Germany) and dissolved in DMSO. Protein kinase C (PKC) inhibitor Gö 16, a synthetic compound structurally related to staurosporine (compound 23 in Hartenstein et al., 1993) and its inactive congener Gö 32 were provided by Dr. C. Schächtele (Gödecke AG, Freiburg, Germany) and dissolved in DMSO. The final DMSO concentration was in each case less than 0.5%.

Recombinant Proteins

cDNAs for *rho*A, Val14-*rho*A, and *rac1* were subcloned into the pGEX-2T vector and recombinant fusion proteins were expressed in *Escherichia coli* and purified as described (Ridley et al., 1992). Briefly, bacteria were sonicated in lysis buffer consisting of 50 mM Tris-HCl, pH 7.5, 50 mM NaCl, 5 mM $MgCl_2$, 1 mM DTT, and 1 mM PMSF. The supernatant (10,000 rpm, 10 min, 4°C) was incubated for 30 min at 4°C with glutathione-agarose beads (Pharmacia Biotech, Freiburg, Germany). The beads were extensively washed with the lysis buffer without PMSF and resuspended in 50 mM Tris-HCl, pH 7.5, 2.5 mM $CaCl_2$, 100 mM NaCl, 5 mM $MgCl_2$, 1 mM DTT. Glutathione-S-transferase (GST) fusion protein was cleaved with thrombin (Sigma) (1.6 U per ml). Beads were pelleted by centrifugation and the supernatant was freed of thrombin by benzamidine–Sepharose (Pharmacia). The recombinant GTP-binding proteins were dialyzed against 100 mM NaCl, 50 mM Tris-HCl (pH 7.5), 5 mM $MgCl_2$ and frozen in aliquots until use.

Preparation of ADP-ribosylated RhoA

250 μl of agarose-coupled GST-RhoA beads were incubated with 10 μl DTT (100 mM), 20 μl NAD (10 mM), 20 μl $MgCl_2$ (100 mM), 50 μl *Clostridium. botulinum* C3 transferase (20 μg/ml), and 650 μl triethanolamine-HCl (25 mM; pH 7.5) for 30 min at ambient temperature. ADP-ribosylated GST-RhoA beads were washed twice with PBS and again with 150 mM NaCl/50 mM triethanolamine-HCl (pH 7.5). RhoA was cleaved from the fusion protein by incubating 250 μl beads with 250 μl thrombin (1.6 U/ml), 150 mM NaCl, 50 mM triethanolamine (pH 7.5), 2.5 mM $CaCl_2$ for 30 min at ambient temperature. ADP-ribosylated RhoA was freed from thrombin by using benzamidine-Sepharose as described above. To test that the preparation was free of C3 transferase, ADP-ribosylated RhoA (1 μg) was added to 1 μg of nonmodified RhoA and incubated for 30 min with 0.1 μM [^{32}P]NAD in the above mentioned ADP-ribosylation buffer without unlabeled NAD. Thereafter, the proteins were analyzed by SDS-PAGE and autoradiography. No labeling of proteins was detected.

cRNA Synthesis

The cDNA for Val14-*rho*A was subcloned into pSP64-poly(A) (Promega) and linearized with EcoRI behind the poly(dT) region of the vector. The plasmids containing the cDNAs for the β1 subunit of the mouse sodium pump (Gloor, 1989) and the α1 subunit of *Torpedo californica* sodium pump (Noguchi et al., 1987) were used as described (Schmalzing et al., 1991*a*). Capped cRNAs were synthesized in vitro with SP6 RNA poly-

merase (Pharmacia), passed through Sephadex G-50 columns (Yisraeli and Melton, 1989), extracted with phenol/chloroform, and recovered by precipitation with salt and ethanol. For efficient translation in oocytes (Schmalzing et al., 1992), the mouse β1 sodium pump subunit cRNA was polyadenylated in vitro by incubation with poly(A) RNA polymerase from *E. coli* (Pharmacia) (Drummond et al., 1985). All the other cRNAs acquired poly(A) tails already during synthesis by transcription of the poly(dT) tails of the cDNA templates. Polyadenylated cRNAs were dissolved in sterile water at a concentration of 0.5 mg/ml, using the optical density reading at 260 nm for quantitation (OD 1.0 = 40 μg/μl).

Microinjection and Maintenance of Oocytes

Xenopus laevis females were obtained directly from South Africa. Follicle cell-free oocytes of oogenesis stages V or VI were obtained as described (Schmalzing et al., 1991*a*) and injected with 46-nl aliquots of toxins, recombinant proteins, or cRNAs as indicated in the figure legends. cRNA-injected oocytes that were cultured for several days were kept at 19°C in sterile oocyte Ringer's solution (1 mM K^+-ORI: 90 mM NaCl, 1 mM KCl, 1 mM $CaCl_2$, and 10 mM Hepes, pH 7.4) supplemented with 1 mM $MgCl_2$ and 50 mg/l gentamycin. The culture medium was changed daily.

In some experiments, oocytes were induced to mature with 1 μM progesterone. Germinal vesicle breakdown was scored by the appearance of a white spot at the animal pole and, occasionally verified by manual dissection of oocytes after fixation in 5% TCA.

ADP Ribosylation

Cytosolic protein extracts from *Xenopus* oocytes were ADP-ribosylated by *botulinum* C3 exoenzyme (Mohr et al., 1990), *limosum* exoenzyme (Just et al., 1992), or *botulinum* C2 toxin (Aktories et al., 1986) as described. Briefly, after the indicated pretreatment, 10 oocytes were frozen in 200 μl of 0.32 M sucrose and 1 mM PMSF. After thawing, the oocytes were homogenized and centrifuged for 10 min at 1,000 *g* and 4°C. The resulting interphase was used for the ADP-ribosylation assay. ADP-ribosylation was performed with 50 mM triethanolamine-HCl (pH 7.5), 2 mM $MgCl_2$, 1 mM DTT, 0.3-1 μM [^{32}P]NAD (~37 kBq) and 0.1 μg/ml C3, 0.1 μg/ml *limosum* exoenzyme or 1 μg/ml C2 toxin (enzyme component C2I), respectively, for 30 min at 37°C in a total volume of 50 μl. Labeled proteins were analyzed by SDS-PAGE and subsequent autoradiography or phosphorimaging (PhosphorImager PSF; Molecular Dynamics, Sunnyvale, CA).

Estimation of the Surface Number and the Total Number of Sodium Pumps

To assess the number of sodium pump molecules of the cell surface, Na^+-loaded oocytes were pulse-labeled for 20 min with 1 μM [^{3}H]ouabain (0.86 TBq/mmol, New England Nuclear) in the presence of 37 kBq/ml [^{14}C]sucrose (Amersham) exactly as described (Schmalzing et al., 1991*a*). Na^+ loading increases the affinity for ouabain and was achieved either by continuous maintenance of oocytes in K^+-free ORI or by a 1-h incubation in a NaCl-based medium without divalent cations just before the ouabain binding assay (Schmalzing et al., 1991*a*) as indicated in the figure legends. To determine the total number of sodium pumps per cell (surface plus internal), oocytes were first permeabilized for 30 min at 5°C and 300 μM digitonin (Schmalzing et al., 1989, 1990) in NaCl-EGTA medium (110 mM NaCl, 1 mM $MgCl_2$, 10 mM EGTA, 10 mM Tris-HCl, pH 7.4) and then incubated at 25°C for 4 h with 0.1 μM [^{3}H]ouabain in NaCl-EGTA (without digitonin) supplemented with 2 mM ATP (sodium salt), pH 7.4. After removal of unbound radioactivity by washing for 1 h at 5°C in NaCl-EGTA under gentle shaking, cells were dissolved individually in 5% SDS and counted in 2 ml of Quickszint 2000 (Zinsser, Frankfurt/Main, Germany). Nonspecific binding was measured with 1 mM unlabeled ouabain and represented less than 5% of total binding. Digitonin (300 μM) did not cause visible damage to the cells.

Estimation of Endocytosis of Sodium Pumps

A rat hybridoma clone secreting mAb brain-specific protein (BSP/3) that recognizes an external epitope on the mouse β1 sodium pump subunit was kindly provided by Dr. C. Goridis (Centre d'Immunologie, INSERM, Marseille, France) (Liabeuf et al., 1984). The IgG was isolated by protein G–Sepharose CL 4B chromatography (Pharmacia) from the supernatant of hybridoma cells and radioiodinated using Na^{125}I (carrier-free, IMS.30; Amersham) and Iodo-Beads™ (Pierce Chem. Oud-Beijerland, The Netherlands) as iodination reagent. Nonincorporated Na^{125}I was removed by filtration of the reaction mix through a Sephadex G-50 spin column. Oocytes expressing exogenous sodium pumps consisting of the mouse β1 subunit and the *Torpedo* α1 subunit (injected with C3 exoenzyme or untreated controls) were labeled with 50 μg/ml of freshly prepared mAb ^{125}I-BSP/3 on ice in oocyte-PBS (30 mM sodium phosphate, 70 mM NaCl, 1 mM $MgCl_2$, 0.1 mM $CaCl_2$). After 1 h, excess antibody was removed by washing in ice-cold ORI. For endocytosis measurements, subsets of these cells were kept on ice as controls or incubated in prewarmed medium (21–23°C). At predetermined times, 10 oocytes per data point were quickly rinsed with ice-cold oocyte-PBS and dissolved individually in 5% SDS. Additional cells were first incubated for 2 min in 25 mM acetic acid in 0.1 M NaCl, pH 2.5, to strip surface-bound ^{125}I-BSP/3 and then dissolved in SDS. The acid treatment has been shown in pilot experiments to release >95% of ^{125}I-BSP/3 from control oocytes kept continuously on ice. Cell-associated radioactivity was determined by liquid scintillation counting. Nonspecific binding was defined as binding of ^{125}I-BSP/3 to oocytes injected with H_2O instead of sodium pump-specific cRNAs, and amounted to 1–2% of total binding to the cRNA-injected cells. Endocytosed ^{125}I-BSP/3 was estimated as the residual radioactivity that could not be eluted by the acid wash at a given time minus the acid-resistant radioactivity associated with cells that were not rewarmed.

Electrophysiological Measurements

Since the sodium pump is electrogenic, pump activity can be expressed as the current generated by the sodium pump. Under maximum stimulating conditions sodium pump current is a measure of the number of sodium pump molecules in the surface membrane. To achieve this, pump current was determined by conventional two-microelectrode voltage clamp as membrane current generated by 5 mM K^+ in Na^+-free solution at a holding potential of −60 mV (Vasilets et al., 1993). To monitor changes in the membrane surface area simultaneous to the sodium pump current, the membrane capacity was determined by integrating the current transients induced by 20 mV depolarizing voltage pulses applied from the holding potential (Vasilets et al., 1990).

Electron Microscopy

For electron microscopy, oocytes incubated under the indicated conditions were fixed at ambient temperature with a fixative consisting of 1.25% glutaraldehyde, 1% formaldehyde, 1 mM $CaCl_2$, 50 mM Hepes/NaOH, pH 7.4. After 3 h, the cells were washed in 0.1 M cacodylate-HCl, pH 7.4, followed by postfixation in 1% OsO_4 in 0.1 M cacodylate-HCl buffer for 1 h at ambient temperature, and overnight block staining with uranyl acetate in H_2O at 4°C. Finally, the cells were dehydrated through a graded ethanol series and, using propylene oxide as an intermedium, embedded in Spurr's resin (Spurr, 1969) or Epon812 (Serva Biochemicals, Heidelberg, Germany). Thin sections were cut with a diamond knife, collected on copper grids, stained with uranyl acetate and lead citrate, and examined in a Siemens 101 Elmiscope.

Fluorescent Labeling of Actin

For localization of actin filaments, cells were fixed in PBS-buffered formaldehyde (10%) for 4 h at room temperature and stored overnight at 4°C in the presence of the fixative. Subsequent incubations were done at room temperature. After two washes with PBS (20 min each), free aldehyde groups were blocked with 2% glycine in PBS for 20 min. Cells were then permeabilized for 30 min in PBS, 0.1% Triton X-100, 1% defatted BSA, and stained for 2 h in the same medium supplemented with 0.5 μM rhodamine-phalloidin. Stained cells were washed three times in PBS containing 0.05% Triton X-100 (20 min each), postfixed for 1 h in PBS-buffered formaldehyde (4%), dehydrated through a graded ethanol series, and embedded in Spurr's resin (Spurr, 1969). Sections cut at 1 μm were viewed and photographed with a Zeiss Axiophot fluorescence microscope.

Miscellaneous

Uptake of [^{3}H]inulin (72 GBq/mmol; Amersham) was determined as described (Vasilets et al., 1990) at ambient temperature (21–23°C).

Unless otherwise indicated, each figure contains representative data given as the means ± SEM of 10–15 separate determinations in individual oocytes from one of at least three reproducible experiments.

Results

C3 Exoenzyme Induces a Translocation of Intracellular Sodium Pumps to the Oocyte Surface

Xenopus oocytes contain similar numbers of sodium pumps both at the cell surface and in intracellular membranes (Schmalzing et al., 1989). Although the surface pumps are continuously endocytosed and recycled to the cell surface, the sizes of the two pump pools do not change significantly over a period of days (Schmalzing et al., 1991*a*). This suggests that the endo- and exocytotic processes that determine the subcellular distribution of sodium pumps are tightly coupled. We monitored the [^{3}H]ouabain binding capacity to study the influence of *botulinum* C3 transferase on endo- and exocytosis. As shown in Fig. 1 *A*, injection of *botulinum* C3 ADP-ribosyltransferase (1 ng/cell) caused a time-dependent increase in ouabain binding, as determined by a 20 min [^{3}H]ouabain pulse that labels ≥97% of surface sodium pumps. Although the results displayed in Fig. 1 *A* suggest that the increase in the number of surface sodium pumps was biphasic, other experiments indicate that the increase is completed within 1 h after the C3 injection. The dose response curve determined 2 h after C3 injection is shown in Fig. 1 *B*. C3 injected at >1 ng/cell induced a maximal increase in the ouabain binding capacity by 60–100%; approximately 20 pg were half-maximally effective. In 19 experiments with oocytes from different females, the increase in the number of surface sodium pumps observed at 1 ng of C3 per cell averaged 76 ± 22% (± SD).

Since a large portion of the recycling pool of sodium pumps of *Xenopus* oocytes resides in the cell interior, it was tempting to attribute the above observations to a redistribution of sodium pumps from intracellular membranes to the plasma membrane. The ouabain binding site of intracellular sodium pumps faces towards the interior of intracellular compartments and can be rendered accessible for [^{3}H]ouabain by nonselective permeabilization of intracellular membranes with SDS (Schmalzing et al., 1989). After permeabilization, the ouabain binding capacity provides an estimate of the total number of sodium pumps per cell. Fig. 2 illustrates that oocytes injected with 1 ng of C3 have the same total number of sodium pumps as control oocytes injected solely with H_2O. Comparison of the total number of pumps with the number of surface pumps indicates that C3 induces a translocation of virtually all intracellular sodium pumps to the cell surface.

C3 Exoenzyme Induces a Simultaneous Increase of Membrane Surface and Sodium Pump Current

We have previously observed that a reduction of the number of surface sodium pumps is associated with a reduction in the surface area of oocytes (Vasilets et al., 1990). To examine whether mobilization of intracellular sodium pumps by C3 exoenzyme reflects an increase in the surface area, we monitored the cell surface area by measuring the electrical capacitance of the oocyte surface membrane. In addition, we measured sodium pump currents in the same cells as an estimate of the number of surface sodium pumps. Results are shown in Fig. 3. At time zero C3 was injected into the oocyte, and after an ~10-min delay, both membrane capacitance and sodium pump current increased with similar time constants of ~15 min (see legend to figure), leading eventually to a 50% increase in surface area and a 88% increase of sodium pump current (Fig. 3 *A*). Assuming a specific membrane capacitance of 1 $\mu F/cm^2$, the change in membrane surface area $\Delta F = F_{max} - F_0$ can be estimated to be about 0.075 cm^2 (F_0 = 0.15 cm^2, F_{max} = 0.225 cm^2). Given that the turnover rate for pump activity is about 50 s^{-1} (Vasilets et al., 1993), the change in the number of surface pump molecules per cell $\Delta N = N_{max} - N_0$ amounted to 6.9×10^9 pump molecules ($N_0 = 3.7 \times 10^9 \equiv$ 250 pumps/μm^2 and $N_{max} = 10.6 \times 10^9 \equiv$ 470 pumps/μm^2). Ouabain binding measurements on C3-injected oocytes from various females yielded very similar results in the number of surface sodium pumps, ranging from 4.2 to 8.3 $\times 10^9$ pump molecules per cell.

C3 Exoenzyme Increases the Number of Sodium Pumps at the Oocyte Surface by Blocking Constitutive Endocytosis

Since sodium pumps cycle continuously between the plasma membrane and intracellular compartments, either acceleration of exocytosis or inhibition of endocytosis could ac-

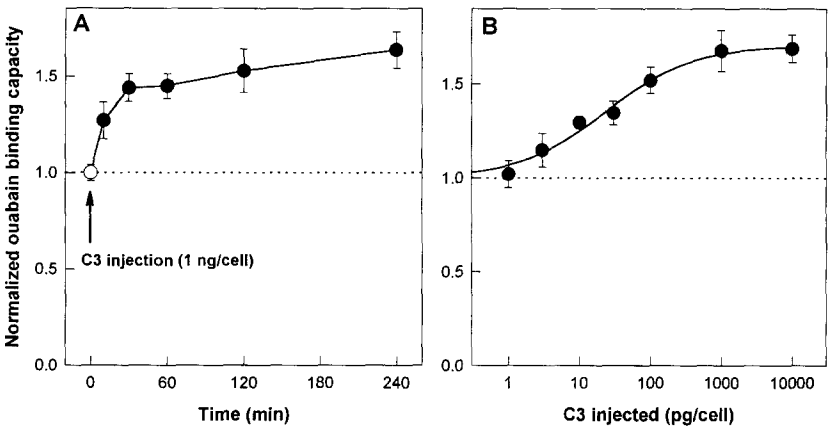

Figure 1. C3 exoenzyme-induced increase of the number of surface sodium pumps. Oocytes were injected with C3 exoenzyme (●) and then assayed for the number of surface sodium pumps, using [^{3}H]ouabain as a ligand. Ouabain binding data were normalized to that of nontreated oocytes of the same batch which were assayed in parallel (○). (*A*) Time course of the C3 effect. Oocytes were loaded with Na^+ by incubation in K^+-free ORI, injected with C3 (1 ng/cell), and subsequently maintained in the same medium for the indicated time. (*B*) Concentration dependence. Oocytes from the same cell batch as in *A* were injected with C3, incubated for 2 h in 1 mM K^+-ORI, and loaded with Na^+ in the Ca^{2+}- and Mg^{2+}-free medium just before the ouabain binding assay. The line drawn through the data points represents a nonlinear least squares fit to a rectangular hyperbola: half-maximal effect at 23 ± 4 pg C3 per cell; maximal increase by 71 ± 4%, corresponding to 6.5 ± 0.4 fmol of ouabain binding sites (S.D. of the least squares fit).

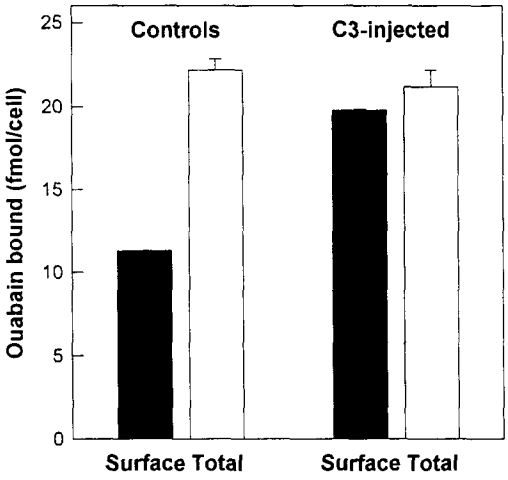

Figure 2. C3 exoenzyme changes the number of surface sodium pumps without net change in the total number of sodium pumps. Oocytes were injected with 10 ng C3 and kept in 1 mM K^+-ORI for 2 h at ambient temperature. One set of cells was loaded with Na^+ by incubation in the NaCl/Tris medium and directly assayed for the number of surface sodium pumps (filled columns). A second set of cells was permeabilized at 10 μM digitonin and assayed for the total number of sodium pumps (surface plus internal, open columns) in the presence of 0.02% SDS and ATP as detailed previously (Schmalzing et al., 1989).

count for the observed mobilization of intracellular sodium pumps. To distinguish between these two possibilities we developed an endocytosis assay based on the cointernalization of a monoclonal antibody bound to surface sodium pumps and the subsequent acid-stripping of noninternalized label. Since monoclonal antibodies that recognize endogenous sodium pumps are not available, we took advantage of the possibility to express by cRNA injection an interspecies hybrid sodium pump in oocytes, consisting of the β1 subunit of the mouse and the α1 subunit of *Torpedo californica* (Schmalzing et al., 1991*a*). Surface-expressed exogenous α1/β1 sodium pump complexes could then be traced by an available mAb, BSP/3, that binds to an ectodomain of the mouse β1 subunit (Liabeuf et al., 1984).

To study the C3 effect on endocytosis, oocytes expressing *Torpedo* α1/mouse β1 sodium pumps at the cell surface were pretreated with the C3 exoenzyme (1 ng/cell) for 2 h and then labeled on ice at a saturating concentration of ^{125}I-BSP/3. Since endocytosis is blocked at 0°C, ^{125}I-BSP/3 bound to the mouse β1 subunit remains on the cell surface as long as the oocytes are kept on ice. To initiate endocytosis, cells were washed and transferred to 21–23°C medium. At various times, oocytes were removed and analyzed for total cell-associated ^{125}I-BSP/3 by liquid scintillation counting. In additional cells, ^{125}I-BSP/3 remaining on the cell surface was stripped by acid wash before liquid scintillation counting. As shown in Fig. 4 *A*, C3-injected oocytes bound ~20% more ^{125}I-BSP/3 than oocytes injected solely with H_2O, most likely as a result of the translocation of intracellular *Torpedo* α1/mouse β1 sodium pumps to the plasma membranes. During incubation, total cell-associated radioactivity declined by 10% as a result of dissociation of surface-bound ^{125}I-BSP/3 (Fig. 4 *A*). Acid-resistant ^{125}I-BSP/3 on cells kept on ice represented 7% of the total cell-associated ^{125}I-BSP/3. On warming, the acid-resistant radioactivity increased at an initial rate of 0.6% of the total cell-associated radioactivity per min (Fig. 4 *B*, controls), most likely because bound ^{125}I-BSP/3 was removed from the cell surface into an acid-resistant, intracellular compartment. Subtraction of acid-resistant radioactivity determined at time zero indicates that at least 30% of the ^{125}I-BSP/3 was in an internal compartment after 90 min. In contrast, in oocytes pre-injected with C3, the internalization of prebound ^{125}I-BSP/3 was greatly delayed (Fig. 4 *B*, *+C3*), suggesting that C3 acts by inhibiting endocytosis of sodium pumps rather than by stimulating their exocytosis.

C3 Does not Block Progesterone-induced Endocytosis of Sodium Pumps

A dramatic change in the number of surface sodium pumps occurs during progesterone-induced meiotic maturation, which prepares oocytes for fertilization. At the time of germinal vesicle breakdown, virtually all sodium pumps are translocated from the cell surface to the interior (Schmalzing et al., 1990). To investigate whether C3 prevents this kind of internalization of sodium pumps, we exposed oocytes injected with 10 ng C3 to 1 μM progesterone to induce maturation. After 16 h at 19°C, cells with the typical white spot at the animal pole (indicative of germi-

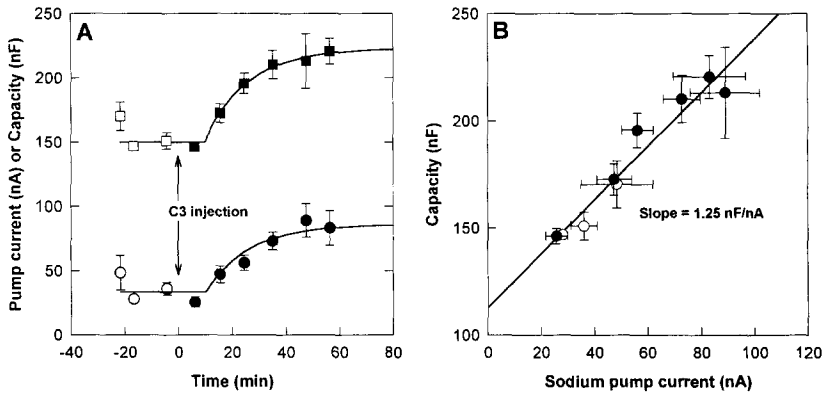

Figure 3. C3 exoenzyme-induced changes of sodium pump current and membrane capacitance. (*A*) Voltage-clamped oocytes were incubated in Na^+- and K^+-free medium. Every 5–15 min, the electrical capacitance of the plasma membrane was determined (*squares*), followed by a perfusion of the test chamber for a few minutes with the same medium supplemented with 5 mM K^+ for maximum activation of the sodium pump. The resulting increase of outward holding current was monitored and taken as the pump-generated current (*circles*). C3 (1 ng/cell) was injected at time zero. Data were fitted by $y = y_{max} - (y_{max} - y_0)e^{\frac{(t-t_0)}{\tau}}$ (with time constant τ = 16 min, delay time t_0 = 10 min). y_0 and y_{max} are 33 and 85 nA, and 150 and 224 nF, respectively. Results are means ± SEM from seven independent experiments. (*B*) Correlation between membrane capacity and sodium pump current. Same data as in *A*.

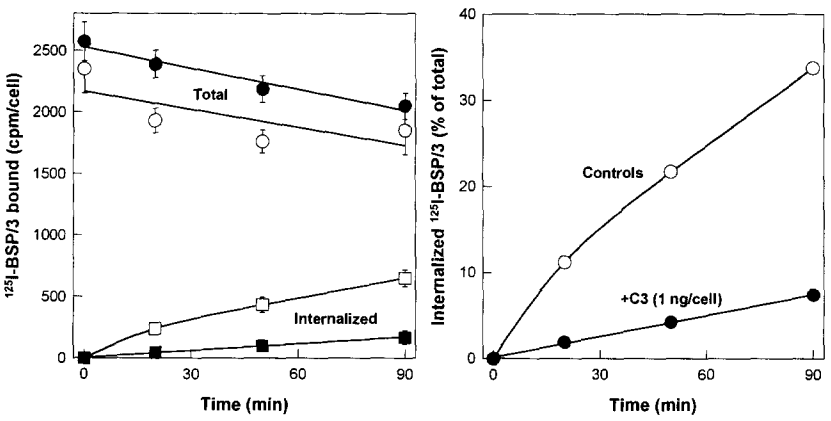

Figure 4. C3 exoenzyme blocks internalization of sodium pumps expressed in oocytes. Oocytes were coinjected with 20 ng of cRNA for the *Torpedo* α1 subunit and 4 ng of cRNA for the mouse β1 subunit. After 3 d at 19°C, the cells were injected with H_2O (*open symbols*) or 1 ng C3 (*filled symbols*), kept for 2 h at 22°C, and then surface labeled for 2 h on ice with freshly iodinated BSP/3. After removal of unbound ligand, the cells were warmed at 22°C, and, at various times, either directly analyzed for total ^{125}I-BSP/3 binding (○, ●) or first incubated for 2 min at pH 2.5 to strip surface-bound ^{125}I-BSP/3 (□, ■) and then analyzed. (*A*) Cell-associated radioactivity before and after the acid wash. (*B*) The amount of ^{125}I-BSP/3 internalized is expressed as a percentage of the total ligand associated with the cells at each time point.

nal vesicle breakdown) were selected, loaded with Na^+, and then assayed for surface binding of [^{3}H]ouabain. C3 treatment neither prevented germinal vesicle breakdown, as verified by sectioning of TCA-fixed oocytes, nor the internalization of the sodium pumps. Oocytes matured in the absence and presence of injected C3 bound 3 ± 2 cpm and 4 ± 3 cpm of [^{3}H]ouabain, respectively, as opposed to 230 ± 12 cpm of [^{3}H]ouabain bound to nonmature oocytes of the same female. The number of intracellular sodium pumps was also identical in oocytes matured in the absence and presence of injected C3 (450 ± 13 cpm vs. 440 ± 18 cpm of bound [^{3}H]ouabain).

C3 Exoenzyme ADP Ribosylates RhoA in Oocytes

C3 exoenzyme is known to ADP-ribosylate small GTP binding proteins of the Rho family (Braun et al., 1989). To examine whether C3 affects Rho in oocytes, subsets of the same C3-treated cells that were also used for the [^{3}H]ouabain binding assay (Fig. 1) were homogenized and incubated with [^{32}P]NAD and C3 (100 ng/ml). Fig. 5 shows that a cytosolic protein of ~20 kD could be radiolabeled, most intensely in oocytes not previously injected with the C3 exoenzyme (lanes *1* and *2*). Analysis of the labeled protein by two-dimensional gel electrophoresis revealed that its isoelectric point is identical with that of RhoA from human platelet membranes (results not shown). This, in conjunction with its cross-reactivity with a polyclonal RhoA-specific anti-peptide antibody (from Santa-Cruz Biotechnology, Santa Cruz, CA) identifies the main substrate for C3 in *Xenopus* oocytes as being RhoA. Pretreatment of intact oocytes with C3 diminished the amount of RhoA protein remaining for subsequent in vitro [^{32}P]ADP-ribosylation in a time- (Fig. 5, lanes *3–7*) and dose-dependent manner (not shown). This indicates that increasing amounts of endogenous RhoA became modified by the prior C3 injection and could therefore not be labeled. The time course of C3-catalyzed ADP-ribosylation of RhoA correlates well with the time-dependent increase in ouabain binding (see Fig. 1 *A* and Fig. 5).

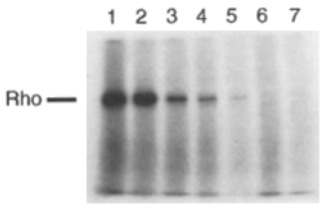

Figure 5. Time course of C3-catalyzed ADP-ribosylation of endogenous Rho in oocytes. Noninjected oocytes (lane *1*) and oocytes injected with H_2O (lane *2*) or C3 (1 ng/cell, lanes *3–7*) were incubated in K^+-free ORI. At the indicated times, subsets of these cells were lysed and ADP-ribosylation was performed as described in the Materials and Methods section. Labeled proteins were analyzed by SDS-PAGE and autoradiography.

ADP-Ribosylated Recombinant RhoA Mimics the Effect of C3 on the Distribution of Sodium Pumps

C. limosum transferase, which ADP-ribosylates the same substrates as C3 (Just et al., 1992) was used to exclude that a contamination of C3 was responsible for the increase in ouabain binding. The *limosum* exoenzyme increased ouabain binding to the same extent as observed with C3 (not shown). To unequivocally demonstrate that ADP-ribosylation of Rho and not of other proteins is responsible for the inhibition of endocytosis, we studied the effect of ADP-ribosylated recombinant RhoA protein, which has been reported to act as a dominant negative inhibitor of endogenous Rho proteins (Paterson et al., 1990). For this purpose, a GST-RhoA fusion protein was isolated and ADP-ribosylated by C3 in vitro. After extensive washing, recombinant RhoA was cleaved by thrombin treatment. ADP-ribosylated RhoA contained no detectable C3 as tested by the incubation of ADP-ribosylated RhoA together with [^{32}P]NAD and unmodified RhoA (results not shown). Even minor traces of contaminating C3 would

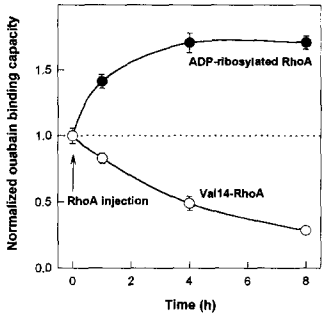

Figure 6. Externalization and internalization of sodium pumps by ADP-ribosylated RhoA and Val14-RhoA, respectively. Oocytes loaded with Na^+ by incubation in K^+-free ORI were injected with 24 ng of ADP-ribosylated RhoA protein or 12 ng of unmodified Val14-RhoA protein. At the indicated times, cells were analyzed for the number of surface sodium pumps.

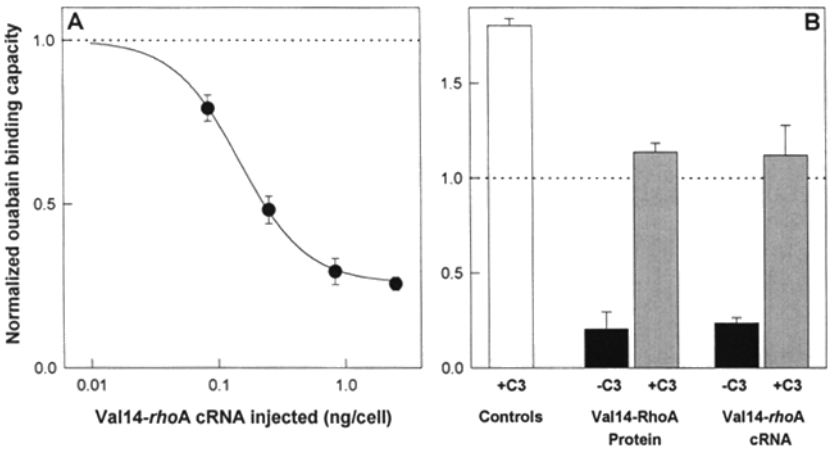

Figure 7. Internalization of surface sodium pumps upon overexpression of Val14-RhoA. (*A*) Oocytes were injected with the indicated amounts of cRNA encoding Val14-*rho*A. After overnight incubation at 19°C, the cells were loaded with Na^+ by incubation in NaCl/Tris medium and then assayed for the number of surface sodium pumps. (*B*) Oocytes were injected with H_2O (controls), 12 ng Val14-Rho A protein, or 12 ng Val14-*rho*A cRNA either alone or together with 10 ng C3 exoenzyme as indicated. After 3 h at 22°C, the cells were loaded with Na^+ by incubation in NaCl/Tris medium and assayed for the number of surface sodium pumps.

give rise to labeling of the added unmodified RhoA. When ADP-ribosylated RhoA was injected into the oocytes we observed a large increase in the ouabain binding capacity (Fig. 6). Comparison with Fig. 1 *A* shows that the increase was slower than that after the C3 injection, but that the maximal increase (60–80%) was of virtually the same magnitude as after the injection of C3.

Overexpression of RhoA Stimulates Endocytosis

Since inactivation of endogenous RhoA by ADP ribosylation or injection of inactivated exogenous RhoA blocked endocytosis of sodium pumps (see Figs. 4 and 6), we anticipated that introduction of exogenous RhoA into oocytes would act in an opposite manner and accelerate endocytosis. Indeed, as also shown in Fig. 6, injection of biologically active recombinant Val14-RhoA protein into oocytes caused a large decrease in the ouabain binding capacity. This effect was particularly marked with the dominantly activated Val14-Rho protein (Fig. 6), but was also observed with normal RhoA (results not shown). Mutation of amino acid 14 from Gly to Val corresponding to the Val12Gly oncogenic mutation in Ras, decreases the intrinsic GTPase activity of RhoA and makes it unresponsive to GTPase-activating proteins, thus preventing its inactivation. A similar decrease in the ouabain binding capacity was also evoked by injection of polyadenylated Val14-*rho*A cRNA into oocytes (Fig. 7 *A*). At high doses of injected RhoA protein or *rho*A cRNA, the plasma membrane of the oocytes became leaky after several h, eventually resulting in cell death. Injection of C3 together with recombinant RhoA or *rho*A cRNA prevented both the disappearance of sodium pumps from the plasma membrane (Fig. 7 *B*) and the oocyte death. Parallel ouabain binding measurements on intact and on detergent-permeabilized oocytes revealed that the overexpression of RhoA caused a translocation of surface sodium pumps to the cell interior with no net change in the total number of sodium pumps (results not shown).

RhoA Stimulates Endocytosis Downstream of PKC

The effects of RhoA on oocytes are very similar to those of activators of PKC such as the diacylglycerol analog PMA, which has also been shown to stimulate fluid-phase endocytosis in oocytes and internalization of sodium pumps (Vasilets et al., 1990). This prompted us to examine if PKC and RhoA were functioning in the same pathway. In agreement with published results, exposure of oocytes to 50 nM PMA induced a rapid disappearance of 70–80% of the sodium pumps from the plasma membrane (Fig. 8). Involvement of PKC can be inferred from the finding that

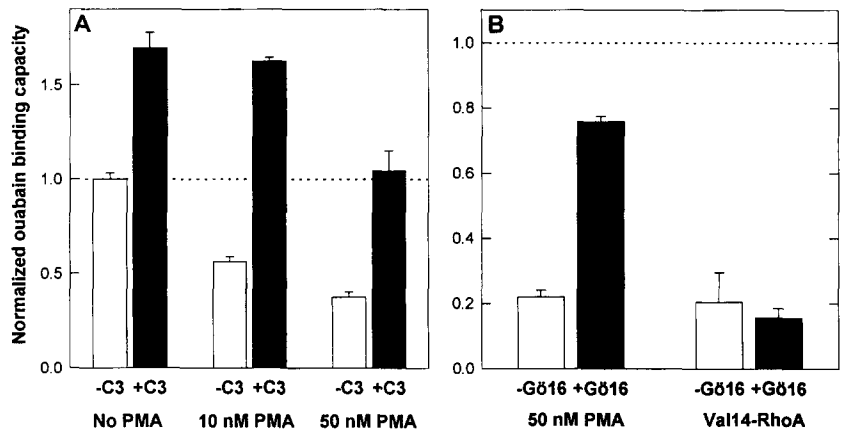

Figure 8. C3 exoenzyme and the PKC inhibitor Gö 16 block PMA-induced internalization of sodium pumps. (*A*) Na^+-loaded oocytes were injected with H_2O (*−C3*) or 20 ng C3 (*+C3*) and kept in K^+-free ORI. After 2 h at 22°C, subsets of these cells were exposed for 50 min to the indicated concentrations of PMA and then assayed for the number of surface sodium pumps. (*B*) Na^+-loaded oocytes were preincubated for at least 15 min at 22°C in K^+-free ORI in the absence (−Gö) or presence of 10 μM Gö 16 (*+Gö16*). Subsets of these cells were then exposed to 50 nM PMA or injected with 12 ng of Val14-RhoA protein as indicated. Following incubation for 50 min (*PMA*) or 2 h (*RhoA*), the number of surface sodium pumps was determined. When indicated Gö 16 was present at all stages of the experiment including the injection of RhoA and the ouabain binding assay. Data were referred to that of control oocytes which were processed in parallel. In untreated oocytes, Gö 16 had no effect on the number of surface sodium pumps.

the PMA effect could be suppressed with Gö 16 (Fig. 8 *B*), a recently identified PKC-specific kinase inhibitor (Hartenstein et al., 1993), but not with Gö 32, an inactive derivative of Gö 16 (results not shown). Most notably, the PMA effect on sodium pump endocytosis was blocked by the introduction of C3 into the oocytes before the addition of PMA (Fig. 8 *A*). This indicates that PMA acts upstream of RhoA to stimulate the internalization of sodium pumps. The failure of Gö 16 to prevent sodium pump internalization caused by the recombinant Val14-RhoA protein (Fig. 8 *B*) or Val14-*rho*A cRNA (not shown) is also compatible with PKC action upstream to RhoA.

We also monitored the uptake of [^{3}H]inulin as a marker of fluid-phase endocytosis to substantiate the involvement of endogenous RhoA in PMA-induced fluid-phase endocytosis. PMA (50–100 nM) induced a two- to fivefold increase in [^{3}H]inulin uptake that was totally blocked with Gö 16, but not with Gö 32, indicating PMA acts upon PKC (results not shown). The time course of the internalization of inulin in the absence and presence of PMA is illustrated in Fig. 9 *A*. PMA-induced inulin uptake displayed biphasic kinetics. After a phase of enhanced uptake, which lasted for 15–45 min, the rate of endocytosis slowed and returned to normal values. Injection of the C3 exoenzyme did not affect basal inulin uptake, but completely blocked the internalization of inulin elicited by a later addition of PMA (Fig. 9 *B*). Furthermore, inactivation of endogenous RhoA by injection of ADP-ribosylated RhoA likewise blocked PMA-induced internalization of inulin (Fig. 9 *B*).

To demonstrate that RhoA affects fluid-phase endocytosis by itself we studied the effect of recombinant RhoA on [^{3}H]inulin uptake. Fig. 10 shows that increasing the activity of RhoA by injection of purified active Val14-RhoA protein stimulated inulin endocytosis by a factor of 2–3. This increase in inulin endocytosis was insensitive to inhibition of PKC with Gö 16 (Fig. 10), corroborating the view that RhoA acts downstream of PKC. The observation that Val14-RhoA–induced fluid-phase endocytosis could be blocked by coinjection of C3 transferase agrees with the results showing that C3 acts specifically on Rho. Injection of C3 alone did not, however, detectably diminish the internalization of inulin (Fig. 9).

Actin is not Involved in the Effects of RhoA or C3 on Endocytosis

Since RhoA is known to affect the actin cytoskeleton, it seemed possible that the effects of RhoA and C3 on endocytosis were secondary to a redistribution of the microfilament network. *Xenopus* oocytes contain a large store of soluble nonmuscle actin in addition to cortical bundles of actin filaments (Franke et al., 1976). We therefore examined the distribution of rhodamine-phalloidin, which binds to filamentous but not to monomeric actin, by fluorescence microscopy. In control oocytes rhodamine-phalloidin revealed a dense network of actin bundles immediately beneath the plasma membrane (Fig. 11 *A*). The orientation of most of the actin bundles was perpendicular to the cell surface and suggests that they are confined to the microvillis. Consistent with lengthening or shortening of the microvilli (see electron micrographs below), the stained cortical sections were broader or thinner in oocytes injected with C3 exoenzyme (Fig. 11 *B*) or RhoA (Fig. 11 *C*), respectively. We conclude from these results that neither C3 nor RhoA profoundly affects actin organization of the oocytes. A profound reorganization of actin took place however upon injection of the enzyme component of *C. botulinum* C2 toxin, C2I, which by ADP-ribosylating G-actin, inhibits actin polymerization (Aktories et

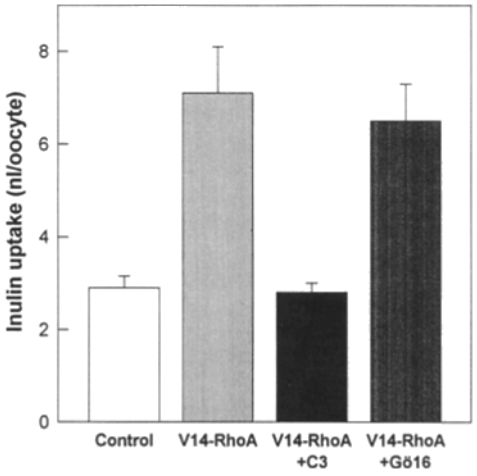

Figure 10. Val14-RhoA stimulates fluid-phase endocytosis. Oocytes were injected with 25 ng Val14-RhoA protein either alone or in combination with 10 ng C3. After a subsequent 60 min interval, the oocytes were allowed to internalize [^{3}H]inulin for 60 min. When indicated 10 μM of the PKC inhibitor Gö 16 was present during all stages of the experiment including the injection of RhoA.

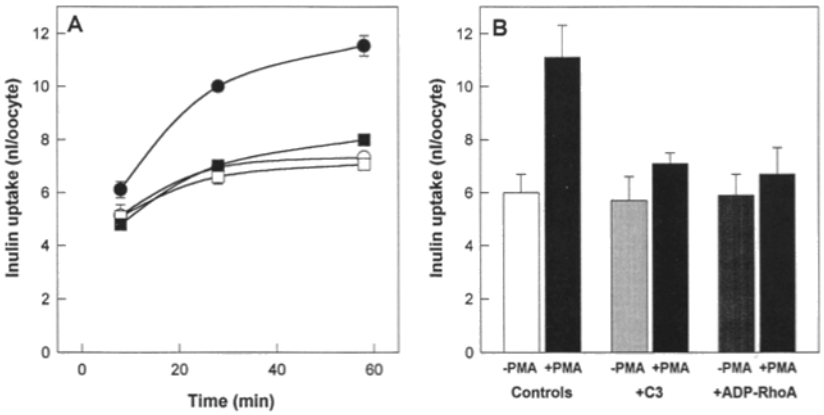

Figure 9. Inactivation of endogenous Rho blocks PMA-induced fluid-phase endocytosis. (*A*) Influence of C3 exoenzyme on PMA-induced internalization of inulin. Oocytes injected or not with C3 (20 ng/cell) were kept for 1 h in K^+-ORI before inulin uptake was initiated in the absence or presence of 50 nM PMA. When indicated, cells were withdrawn and analyzed for internalized inulin. ○ Controls; ● 50 nM PMA; □ C3 alone; ■ C3 + 50 nM PMA. (*B*) Oocytes were injected with H_2O (*Controls*), 20 ng C3, or 25 ng ADP-ribosylated RhoA. After 2 h at 22°C, inulin uptake was initiated in the absence (*−PMA*) or presence of 50 nM PMA (*+PMA*) and stopped after 1 h by washing the cells as above.

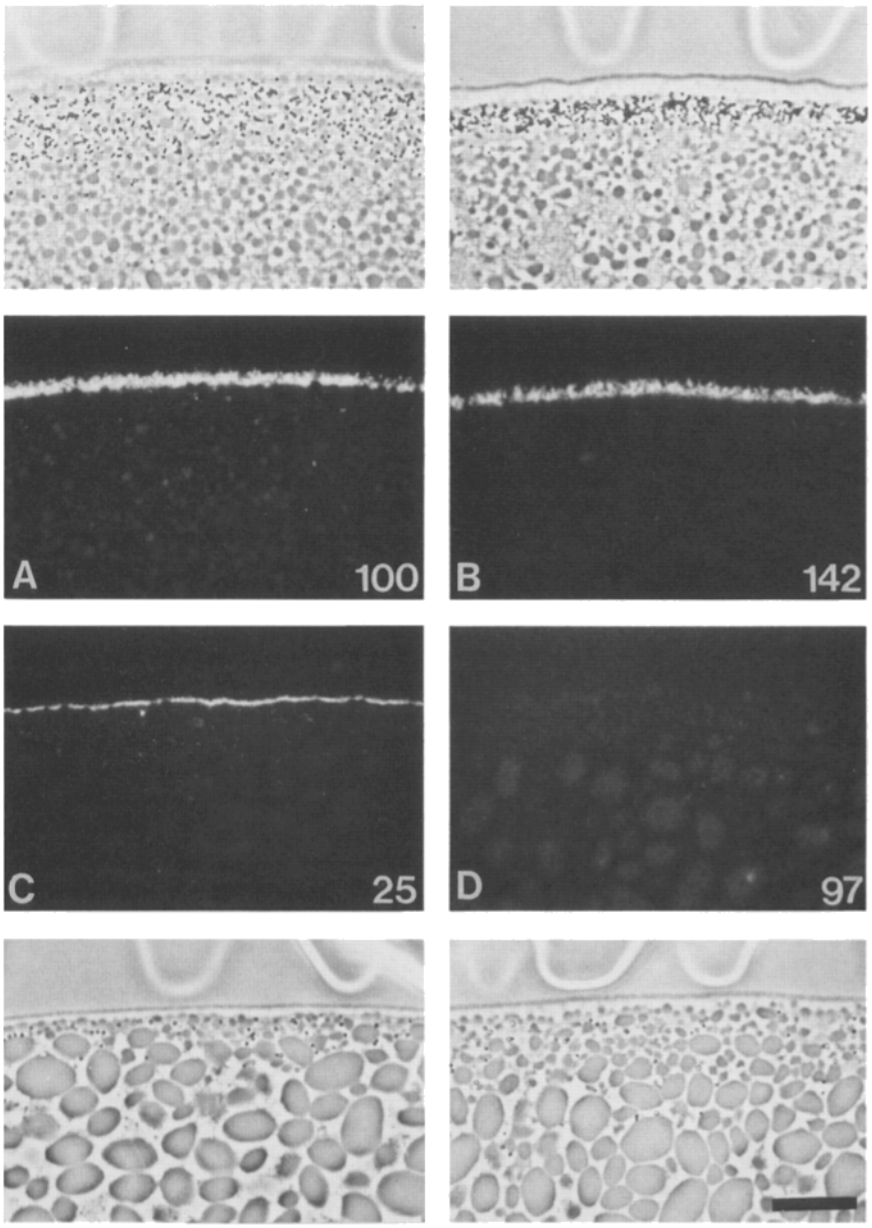

Figure 11. Fluorescence micrographs of actin filaments in oocytes. Oocytes were injected with H_2O (*A*), 10 ng C3 exoenzyme (*B*), 23 ng *rhoA* cRNA (*C*), or 1.6 ng C2I (*D*), and kept for 4 h at ambient temperature. Following fixation with formaldehyde, actin was stained using rhodamine-conjugated phalloidin. The numbers in the lower right corner of the figures give an estimate of the percentage of surface sodium pumps at the time of fixation relative to those of the control oocytes. These data were derived from ouabain binding measurements on subsets of the oocytes used for visualization of actin. Upper and lower photographs: phase-contrast photographs of the fluorescence images. Bars, 10 μm.

al., 1986; Aktories et al., 1986, 1992). Consistent with a complete depolymerization of actin C2I-injected oocytes totally lacked cortical actin bundles (Fig. 11 *D*). A complete modification of actin under these experimental conditions was demonstrated by the in vitro ADP-ribosylation of delipidated lysate from C2 toxin-injected oocytes with [^{32}P]NAD and new C2 toxin (1 μg/ml). As shown in Fig. 12 *A* (lanes *5* and *6*), a polypeptide of 43 kD (actin) was radiolabeled in control oocytes, while no labeling of actin could be detected when oocytes were treated with C2I before lysis (lanes *7* and *8*). Surprisingly, despite this dramatic change in actin organization, C2I had virtually no effect on either sodium pump distribution (results not shown) or basal and PMA-induced internalization of inulin (Fig. 12 *B*).

Ultrastructural Changes of Oocyte Surface Induced by RhoA and C3

To visualize changes in the surface structure that may account for the changes in the number of surface sodium pumps, control oocytes as well as oocytes injected with *rhoA* cRNA or C3 were processed for electron microscopy. Fig. 13 *A* shows that the surface of control oocytes is covered with numerous partially branched microvilli. In contrast, oocytes injected with *rhoA* cRNA have lost most of their microvilli (Fig. 13 *B*) but retained their normal pigmentation on light microscopic level. Similar ultrastructural changes of the surface structure have been previously detected on oocytes treated with PMA and shown by membrane capacitance measurements to result from a 70–80% decrease of the surface area (Vasilets et al., 1990). Since C3 injection increases membrane capacitance (Fig. 3), we expected to observe an increase in the length of microvilli in such cells. Indeed, electron microscopy revealed that C3-injected oocytes are covered with elongated and convoluted microvilli (Fig. 13, *C* and *D*). We did not quantify these changes as the enlargement of the cell surface was easily visible. Ouabain binding data indicate that 1 ng

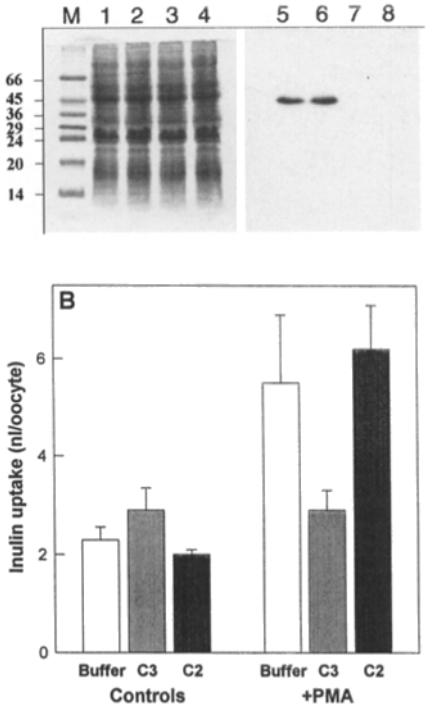

Figure 12. Depolymerization of oocyte actin by *C. botulinum* C2I toxin. (*A*) ADP-ribosylation of actin by C2I. Oocytes injected with C2 toxin (lanes *3*, *4*, *7*, and *8*) or solely with buffer (lanes *1*, *2*, *5*, and *6*) were kept for 1 h at 22°C before subsets of the cells were treated as indicated with PMA. After an additional 1 h at 22°C, delipidated lysates were prepared and ADP-ribosylated with [^{32}P]NAD and 1 μg/ml C2 toxin. Labeled proteins were analyzed by SDS-PAGE and autoradiography. *M*, molecular mass markers (in kD). (*B*) Influence of C2I on PMA-induced internalization of inulin. Oocytes were injected with H_2O, 40 ng C3, or 5 ng C2I as indicated. After preincubation intervals lasting 1 (C2) or 2 h (C3), the oocytes were allowed to internalize [^{3}H]inulin for 60 min in the absence (controls) and presence of 50 nM PMA (*+PMA*).

C3 per cell increased the number of surface sodium pumps by 59% in these oocytes.

Discussion

A Role for RhoA in Endocytosis

The present study establishes a role for RhoA in membrane traffic in *Xenopus* oocytes on the basis of the following observations. (*a*) Injection of normal or mutationally activated RhoA protein induced a rapid and marked decrease of both the surface area and the number of surface pumps, accompanied by increased fluid-phase endocytosis. (*b*) Exactly the same changes, albeit with a slower rate, were elicited by injection of *rho*A cRNA. This excludes any possibility that the observed effects were due to a contaminant such as salt or GTPγS in the injected protein preparations. (*c*) The inactivation of endogenous RhoA by injection of C3 exoenzyme or ADP-ribosylated recombinant RhoA led to the opposite effect, an increase in the surface area and number of cell surface sodium pumps. Although C3 has been reported to ribosylate Rac proteins, at least in vitro (Didsbury et al., 1989), an involvement of Rac in the observed effects of C3 can be ruled out since recombinant Rac1 did not affect the number of surface sodium pumps of oocytes (results not shown). Moreover, ribosylation of Rac by C3 has been shown to require detergent, and is therefore unlikely to play a role in vivo (Just et al., 1992). Other Ras-like proteins do not serve as substrates for C3 (Ridley and Hall, 1992). (*d*) The C3-analogous effect of ADP-ribosylated exogenous RhoA is in agreement with previous findings showing that ADP-ribosylation turns Rho into a dominant negative configuration (Ridley and Hall, 1992). Consequently, the efficacy of ADP-ribosylated RhoA indicates that endogenous RhoA is itself involved in the observed effects. In addition, these experiments show that the effect of C3 can be entirely attributed to ribosylation and inactivation of endogenous RhoA.

Changes in the surface area and the number of surface sodium pumps could result from changes either in the rate of externalization and/or the rate of internalization. The stimulation of fluid-phase endocytosis by activated RhoA and the inhibition of constitutive endocytosis of expressed sodium pumps by inactivation of RhoA both provide clear evidence that RhoA affects endocytosis rather than exocytosis. Our findings can easily be reconciled with the view that RhoA acts as a molecular switch and triggers endocytosis in its active GTP-bound form, while endocytosis ceases when RhoA is inactive. Although sodium pump distribution and surface area changed in response to the various treatments as predicted by this model, we were unable to demonstrate the expected decrease in basal fluid-phase endocytosis of inulin upon inactivation of endogenous RhoA. The reason for this discrepancy remains to be determined.

RhoA Acts not Only on Actin

There is substantial evidence that the members of the Rho/Rac family are involved in a variety of actomyosin-dependent phenomena including changes of cell shape (Paterson et al., 1990), cell motility (Takaishi et al., 1993), smooth muscle contraction (Hirata et al., 1992), and cell division of *Xenopus* embryos (Kishi et al., 1993). The persistently active Val14-Rho protein was shown to induce a dramatic polymerization of actin in starved cells (Paterson et al., 1990; Ridley and Hall, 1992), while inactivation of Rho by C3 transferase inhibited stress fiber formation and caused a destruction of the actin cytoskeleton (Chardin et al., 1989; Paterson et al., 1990; Ridley and Hall, 1992; Wiegers et al., 1991). Additional evidence that Rho has an important role in the regulation of the actin cytoskeleton stems from the observation that C3-like effects can be elicited by another ADP-ribosyltransferase, C2 (Paterson et al., 1990), which ADP-ribosylates actin monomers directly and blocks their polymerization (Aktories et al., 1986; Wille et al., 1992). Microfilaments have also been implicated in fluid-phase and/or receptor-mediated endocytosis (Kübler and Riezman, 1993; Gottlieb et al., 1993). It therefore seemed reasonable to suppose that RhoA acts through actin to regulate endocytosis in *Xenopus* oocytes. Our experimental evidence argues against a predominant role of actin in RhoA-regulated endocytosis. Firstly, direct inhibition of actin polymerization by the C2 transferase com-

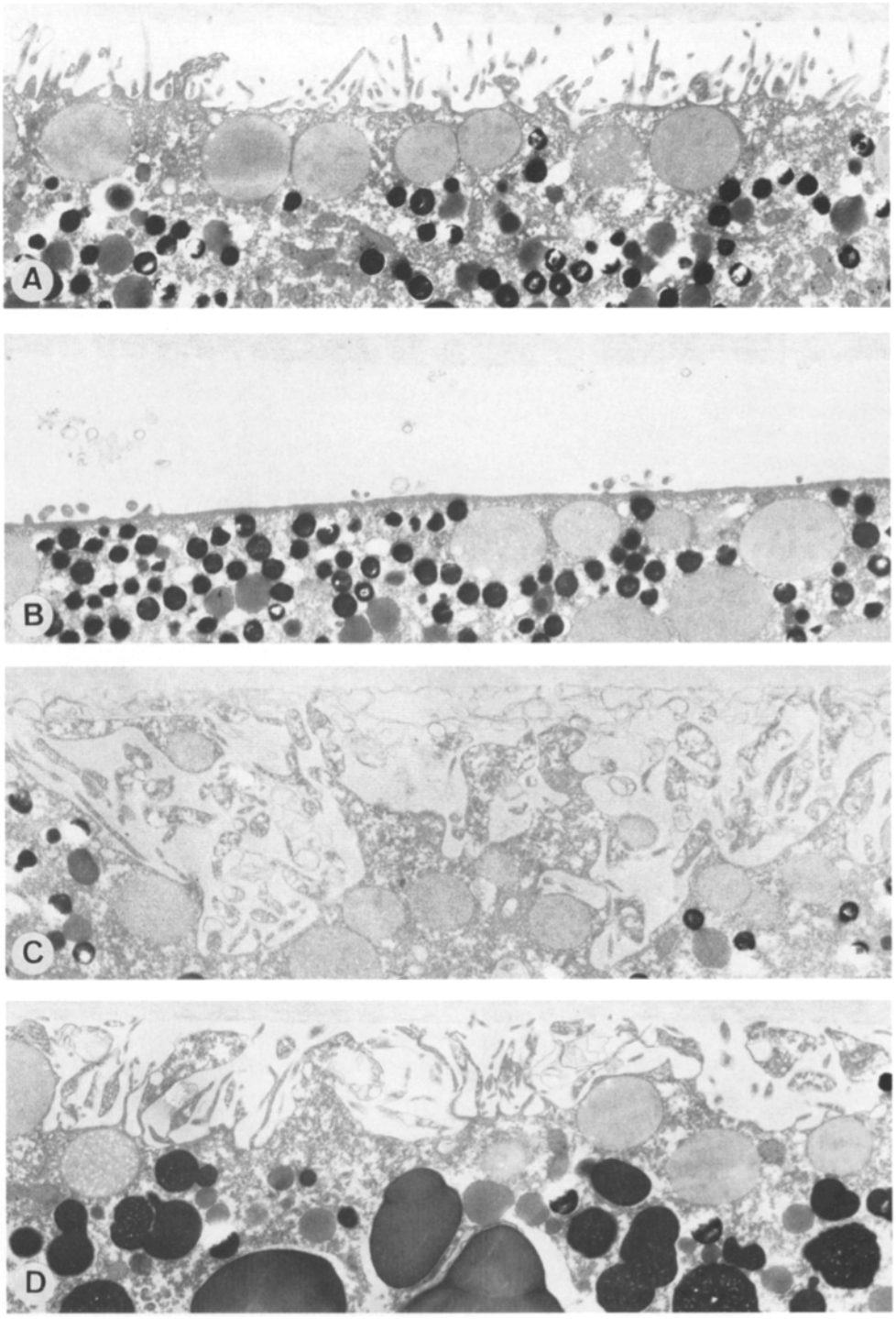

Figure 13. Cortical aspects of oocytes after inactivation or overexpression of RhoA. Noninjected oocytes (*A*) and oocytes injected with 23 ng Val14-*rho*A cRNA (*B*) or 1 ng C3 exoenzyme (*C* and *D*) were kept for 4 h at 22°C and then fixed and processed for electron microscopy as described in Materials and Methods. (*A–C*) animal pole; (*D*) vegetal pole. Bar, 1 μm.

pletely failed to mimic the C3 effect and to affect endocytosis in *Xenopus* oocytes; and secondly, C3 injection did not grossly change the distribution of rhodamine-phalloidin–stained actin filaments in oocytes. Analogous to the behavior of other Ras-like proteins such as Rab proteins, we suggest that the GTP-bound form of RhoA can associate with membranes to enhance the budding of endocytotic vesicles. Remarkably, such a function would agree with the recently determined localization of human RhoB on early endosomes of rat-2 cells (Adamson et al., 1992).

RhoA is Involved in Constitutive, But Not in Progesterone-induced Internalization of Sodium Pumps

Sodium pumps appear to be subjected to constitutive and regulated endocytosis in *Xenopus* oocytes (for a recent review see Schmalzing, 1994). A constitutive type of endocytosis takes place in prophase-arrested oocytes, when oocytes continuously recycle sodium pumps. Our results suggest that it is exactly this type of sodium pump internalization that is regulated by Rho. We surmise that the addi-

tional sodium pumps that appear at the plasma membrane after blockade of endocytosis by C3 represent the internal portion of the recycling pool of sodium pumps. The large increase in surface membrane area and sodium pumps induced by C3 agrees with our concept that oocytes contain a large stockpile of internal membranes and sodium pumps (Schmalzing et al., 1990). Inactivation of RhoA may cause a premature recruitment of stored constituents which may normally serve for the formation of new (interblastomeric) plasma membranes after fertilization. The recent observation that RhoA is required for cleavage formation in Xenopus embryos (Kishi et al., 1993) would support such a hypothesis.

Sodium pump internalization combined with a large reduction of the surface area (Kado et al., 1981) also occurs during progesterone-induced meiotic maturation (Schmalzing et al., 1990). However, despite apparent similarities to PMA- and RhoA-induced endocytosis, meiotic maturation does not lead to enhanced fluid-phase endocytosis and the extent of sodium pump internalization is also strikingly different. After exposure to progesterone, virtually all the sodium pumps disappear from the plasma membrane (Schmalzing et al., 1990). In contrast, after PMA or RhoA treatment, the number of surface sodium pumps never declined under 20% of its initial value. From the proportional changes of the surface area, we conclude that the reduction of surface sodium pumps in response to PMA or RhoA is limited by the minimum surface area of an oocyte that has lost all its microvilli and resembles a smooth ball. Altogether, we attribute the incomplete removal of surface sodium pumps to constitutive, nonselective endocytosis, as opposed to progesterone-regulated endocytosis which seems to comprise selective retrieval of sodium pumps from the plasma membrane (Schmalzing, 1994). The view that PMA/RhoA-induced endocytosis and progesterone-induced endocytosis are fundamentally different is further supported by the observation that inactivation of endogenous RhoA by C3 exoenzyme failed to block progesterone-induced internalization of sodium pumps.

RhoA-mediated Constitutive Endocytosis is Clathrin-independent

Internalization of many recycling receptors is clathrin-dependent and can be blocked efficiently by potassium depletion that removes clathrin-coated pits from the plasma membrane. In addition to this well characterized pathway, there is evidence for an alternative clathrin-independent endocytotic pathway that continues to operate even after potassium depletion (Sandvig and van Deurs, 1994). Because K^+ depletion may affect endocytosis, it is of interest that the ouabain binding measurements were for methodological reasons performed on oocytes depleted of K^+ by the Na^+ loading procedure (Schmalzing et al., 1991*a*). Comparison of the data presented in Fig. 1 shows that K^+ depletion has no effect on internalization and externalization of sodium pumps since virtually identical results were obtained irrespective of whether C3 and RhoA were introduced into K^+-depleted oocytes (Fig. 1 *A*) or oocytes with normal internal K^+ (Fig. 1 *B*). In the later case, Na^+ loading was performed immediately before the ouabain binding assay. We conclude from these data that RhoA-regulated internalization of sodium pumps is mediated by clathrin-independent endocytosis.

PKC and RhoA

PMA stimulates fluid-phase endocytosis in various cell systems including *Xenopus* oocytes by activating PKC. As shown here, PMA-induced endocytosis is blocked by C3 and ADP-ribosylated RhoA indicating that PKC acts through Rho upon endocytosis. A similar signal transduction pathway, with RhoA located downstream of PKC, has been postulated from the inhibitory effect of C3 on PKC-induced platelet activation (Morii et al., 1992) and lymphocyte aggregation (Tominaga et al., 1993). Furthermore, in KB cells, PMA has been shown to induce membrane ruffling by a mechanism involving RhoA (Nishiyama et al., 1994). Since membrane ruffling and pinocytosis are closely related events, the PMA- or RhoA-induced reorganization of the oocyte surface can be considered to represent the oocyte phenotype of membrane ruffling of cultured cells. The finding that RhoA reduces the number of actin fibers in oocytes is contradictory to this view, because RhoA-induced membrane ruffles in KB cells are clearly associated with newly formed actin fibers. PMA also activates membrane ruffling in Swiss 3T3 cells, but in these cells Rac, and not Rho proteins are involved (Ridley et al., 1992). Moreover, Hall and coworkers have proposed that PMA inhibits the signal pathway that activates RhoA by LPA or bombesin (Ridley and Hall, 1994). It remains to be clarified whether the apparently different regulatory effects of PMA depend on specific PKC isoforms.

Direct activation of Rho by PKC seems unlikely to account for the observed effects, since the deduced amino acid sequence of Rho does not contain a consensus sequence for PKC-dependent phosphorylation. Therefore other factors must communicate the activatory signal to RhoA. RhoA-activating guanine-nucleotide exchange factors are possible candidates (reviewed by Boguski and McCormick, 1993). These proteins share a region of similarity, designated the Dbl domain, that has been recently shown to stimulate the release of GDP from Rho-like proteins (Hart et al., 1994). Indirect evidence for an involvement of protein phosphorylation in the regulation of Rho comes from the recent observation that the phosphorylation of Rho-regulating factors alters the ability of Rho to serve as an ADP-ribosylation substrate for C3 (Fritz and Aktories, 1994).

Taken together, our results assign RhoA a role in fluid-phase endocytosis and recycling of membrane proteins. In *Xenopus* oocytes at least, RhoA seems not to be significantly involved in the organization of the actin cytoskeleton nor is actin itself involved in endocytosis. The downstream activation of RhoA by PKC suggests the existence of a signaling pathway in which activation results in an increase in endocytotic activity and eventually in a profound change in the cell surface structure. The physiological ligands of this pathway that may be capable of regulating endocytotic activity in *Xenopus* oocytes remain to be identified.

We thank the following scientists for generous gifts of probes: Dr. C. Goridis for the hybridoma producing mAb BSP/3, Dr. S. Gloor and Dr. M. Kawamura for the cDNAs encoding the mouse β1 sodium pump sub-

unit and the *Torpedo* α1 sodium pump subunit, respectively. The excellent technical assistance of M. Lerner, G. Kiefer, and S. Drewing is gratefully acknowledged. We thank Dr. L. Griffith, University of Bonn, Institut für Anatomie, Physiologie und Hygiene der Haustiere, for helpful linguistic comments.

This work was supported by grants of the Deutsche Forschungsgemeinschaft (SFB 246, project B10, to K. Aktories; SFB 169, project A8, to G. Schmalzing).

Received for publication 3 January 1995 and in revised form 15 May 1995.

References

Abo, A., E. Pick, A. Hall, N. Totty, C. G. Teahan, and A. W. Segal. 1991. Activation of the NADPH oxidase involves the small GTP-binding protein $p21^{rac1}$. *Nature (Lond.).* 353:668–670.

Adamson, P., H. F. Paterson, and A. Hall. 1992. Intracellular localization of the $p21^{rho}$ proteins. *J. Cell Biol.* 119:617–627.

Aktories, K., M. Bärmann, I. Ohishi, S. Tsuyama, K. H. Jakobs, and E. Habermann. 1986. Botulinum C2 toxin ADP-ribosylates actin. *Nature (Lond.).* 322:390–392.

Aktories, K., U. Weller, and G. S. Chhatwal. 1987. *Clostridium botulinum* type C produces a novel ADP-ribosyltransferase distinct from botulinum C2 toxin. *FEBS Lett.* 212:109–113.

Aktories, K., S. Rösener, U. Blaschke, and G. S. Chhatwal. 1988. Botulinum ADP-ribosyltransferase C3. Purification of the enzyme and characterization of the ADP-ribosylation reaction in platelet membranes. *Eur. J. Biochem.* 172:445–450.

Aktories, K., M. Wille, and I. Just. 1992. Clostridial actin ADP-ribosylating toxins. *Current Top. Microbiol Immunol.* 175:97–113.

Bar-Sagi, D., F. McCormick, R. J. Milley, and J. R. Feramisco. 1987. Inhibition of cell surface ruffling and fluid-phase pinocytosis by microinjection of anti-*ras* antibodies into living cells. *J. Cell. Physiol. Suppl.* 5:69–73.

Boguski, M. S., and F. McCormick. 1993. Proteins regulating Ras and its relatives. *Nature (Lond.).* 366:643–654.

Boman, A. L., T. C. Taylor, P. Melançon, and K. L. Wilson. 1992. A role for ADP-ribosylation factor in nuclear vesicle dynamics. *Nature (Lond.).* 358: 512–514.

Braun, U., B. Habermann, I. Just, K. Aktories, and J. Vandekerckhove. 1989. Purification of the 22 kDa protein substrate of botulinum ADP-ribosyltransferase C3 from porcine brain cytosol and its characterization as a GTP-binding protein highly homologous to the *rho* gene product. *FEBS Lett.* 243:70–76.

Bucci, C., R. G. Parton, I. H. Mather, H. Stunnenberg, K. Simons, B. Hoflack, and M. Zerial. 1992. The small GTPase rab5 functions as a regulatory factor in the early endocytotic pathway. *Cell.* 70:715–728.

Chardin, P., P. Boquet, P. Madaule, M. R. Popoff, E. J. Rubin, and D. M. Gill. 1989. The mammalian G protein *rhoC* is ADP-ribosylated by *Clostridium botulinum* exoenzyme C3 and affects actin microfilaments in Vero cells. *EMBO J.* 8:1087–1092.

Chavrier, P., R. G. Parton, H. P. Hauri, K. Simons, and M. Zerial. 1990. Localization of low molecular weight GTP binding proteins to exocytic and endocytic compartments. *Cell.* 62:317–329.

Didsbury, J., R. F. Weber, G. M. Bokock, T. Evans, and R. Synderman. 1989. *rac*, a novel *ras*-related family of proteins that are botulinum toxin substrates. *J. Biol. Chem.* 264:16378–16382.

Donaldson, J. G., D. Cassel, R. A. Kahn, and R. D. Klausner. 1992. ADP-ribosylation factor, a small GTP-binding protein, is required for binding of the coatomer protein β-COP to Golgi membranes. *Proc. Natl. Acad. Sci. USA.* 89:6408–6412.

Drummond, D. R., J. Armstrong, and A. Colman. 1985. The effect of capping and polydenylation on the stability, movement and translation of synthetic messenger RNAs in *Xenopus* oocytes. *Nucl. Acids Res.* 13:7375–7394.

Ferro-Novick, S., and P. Novick. 1993. The role of GTP-binding proteins in transport along the exocytic pathway. *Annu. Rev. Cell Biol.* 9:575–599.

Fischer v. Mollard, G., G. A. Mignery, M. Baumert, M. S. Perin, T. J. Hanson, P. M. Burger, R. Jahn, and T. C. Südhof. 1990. rab3 is a small GTP-binding protein exclusively localized to synaptic vesicles. *Proc. Nat. Acad. Sci. USA.* 87:1988–1992.

Fischer von Mollard, G., T. C. Südhof, and R. Jahn. 1991. A small GTP-binding protein dissociates from synaptic vesicles during exocytosis. *Nature (Lond.).* 349:79–81.

Fischer von Mollard, G., B. Stahl, C. Li, T. C. Südhof, and R. Jahn. 1994. Rab proteins in regulated exocytosis. *Trends Biochem. Sci.* 19:164–168.

Franke, W. W., P. C. Rathke, E. Seib, M. F. Trendelenburg, M. Osborn, and K. Weber. 1976. Distribution and mode of arrangement of microfilamentous structures and actin in the cortex of the amphibian oocyte. *Cytobiologie.* 14: 111–130.

Fritz, G., and K. Aktories. 1994. ADP-ribosylation of Rho proteins by *Clostridium botulinum* exoenzyme C3 is influenced by phosphorylation of Rho-associated factors. *Biochem. J.* 300:133–139.

Gloor, S. 1989. Cloning and nucleotide sequence of the mouse Na,K-ATPase β-subunit. *Nucl. Acids Res.* 17:10117.

Gottlieb, T. A., I. E. Ivanov, M. Adesnik, and D. D. Sabatini. 1993. Actin microfilaments play a critical role in endocytosis at the apical but not the basolateral surface of polarized epithelial cells. *J. Cell Biol.* 120:695–710.

Gruenberg, J., and M. J. Clague. 1992. Regulation of intracellular membrane transport. *Curr. Opin. Cell Biol.* 4:593–599.

Hart, M. J., A. Eva, D. Zangrilli, S. A. Aaronson, T. Evans, R. A. Cerione, and Y. Zheng. 1994. Cellular transformation and guanine nucleotide exchange activity are catalyzed by a common domain on the *dbl* oncogene product. *J. Biol. Chem.* 269:62–65.

Hartenstein, J. H., J. Aranda, H. Barth, H. J. Betche, J. Kleinschroth, R. Reck, C. Rudolph, U. Trostmann, and C. Schächtele. 1993. The design of protein kinase C inhibitors. *In* Perspectives in Medicinal Chemistry. B. Testa, E. Kyburz, W. Fuhrer, and R. Giger, editors. Verlag Helvetica Chimica Acta, Basel. 99–118.

Haubruck, H., C. Disela, P. Wagner, and D. Gallwitz. 1987. The *ras*-related *ypt* protein is an ubiquitous eukaryotic protein: isolation and sequence analysis of mouse cDNA clones highly homologous to the yeast *YPT1* gene. *EMBO J.* 6:4049–4053.

Hirata, K., A. Kikuchi, T. Sasaki, S. Kuroda, K. Kaibuchi, Y. Matsuura, H. Seki, K. Saida, and Y. Takai. 1992. Involvement of *rho* p21 in the GTP-enhanced calcium ion sensitivity of smooth muscle contraction. *J. Biol. Chem.* 267: 8719–8722.

Just, I., C. Mohr, G. Schallehn, L. Menard, J. R. Didsbury, J. Vandekerckhove, J. van Damme, and K. Aktories. 1992. Purification and characterization of an ADP-ribosytransferase produced by *Clostridium limosum*. *J. Biol. Chem.* 267:10274–10280.

Kado, R. T., K. Marcher, and R. Ozon. 1981. Electrical membrane properties of the *Xenopus laevis* oocyte during progesterone-induced meiotic maturation. *Dev. Biol.* 84:471–476.

Kahn, R. A., P. Randazzo, T. Serafini, O. Weiss, C. Rulka, J. Clark, M. Amherdt, P. Roller, L. Orci, and J. E. Rothman. 1992. The amino terminus of ADP-ribosylation factor (ARF) is a critical determinant of ARF activities and is a potent and specific inhibitor of protein transport. *J. Biol. Chem.* 267: 13039–13046.

Keller, H. U. 1990. Diacylglycerols and PMA are particularly effective stimulators of fluid pinocytosis in human neutrophils. *J. Cell. Physiol.* 145:465–471.

Kishi, K., T. Sasaki, S. Kuroda, T. Itoh, and Y. Takai. 1993. Regulation of cytoplasmic division of *Xenopus* embryo by *rho* p21 and its inhibitory GDP/GTP exchange protein (*rho* GDI). *J. Cell Biol.* 120:1187–1195.

Knaus, U. G., P. G. Heyworth, T. Evans, J. T. Curnutte, and G. M. Bokoch. 1991. Regulation of phagocyte oxygen radical production by the GTP-binding protein Rac 2. *Science (Wash. DC).* 254:1512–1515.

Kübler, E., and H. Riezman. 1993. Actin and fimbrin are required for the internalization step of endocytosis in yeast. *EMBO J.* 12:2855–2862.

Lenhard, J. M., R. A. Kahn, and P. D. Stahl. 1992. Evidence for ADP-ribosylation factor (ARF) as a regulator of *in vitro* endosome-endosome fusion. *J. Biol. Chem.* 267:13047–13052.

Liabeuf, A., J.-P. Gorvel, and C. Goridis. 1984. Recognition of sodium- and potassium-dependent adenosine triphosphatase of mouse lymphoid cells by means of a monoclonal antibody. *Cell Tissue Res.* 238:253–261.

Madaule, P., and R. Axel. 1985. A novel *ras*-related gene family. *Cell.* 41:31–40.

Miura, Y., A. Kikuchi, T. Musha, S. Kuroda, H. Yaku, T. Sasaki, and Y. Takai. 1993. Regulation of morphology by *rho* p21 and its inhibitory GDP/GTP exchange protein (*rho* GDI) in Swiss 3T3 cells. *J. Biol. Chem.* 268:510–515.

Mohr, C., I. Just, A. Hall, and K. Aktories. 1990. Morphological alterations of *Xenopus* oocytes induced by valine-14 $p21^{rho}$ depend on isoprenylation and are inhibited by *Clostridium botulinum* C3 ADP-ribosyltransferase. *FEBS Lett.* 275:168–172.

Morii, N., T. Teru-uchi, T. Tominaga, N. Kumagai, S. Kozaki, F. Ushikubi, and S. Narumiya. 1992. A *rho* gene product in human blood platelets. II. Effects of the ADP-ribosylation by botulinum C3 ADP-ribosyltransferase on platelet aggregation. *J. Biol. Chem.* 267:20921–20926.

Nishiyama, T., T. Sasaki, K. Takaishi, M. Kato, H. Yaku, K. Araki, Y. Matsuura, and Y. Takai. 1994. *rac* p21 is involved in insulin-induced membrane ruffling and *rho* p21 is involved in hepatocyte growth factor- and 12-*O*-tetradecanoylphorbol-13-acetate (TPA)-induced membrane ruffling in KB cells. *Mol. Cell. Biol.* 14:2447–2456.

Noguchi, S., M. Mishina, M. Kawamura, and S. Numa. 1987. Expression of functional ($Na^+ + K^+$)-ATPase from cloned cDNAs. *FEBS Lett.* 225:27–32.

Novick, P., and P. Brennwald. 1993. Friends and family: the role of the Rab GTPases in vesicular traffic. *Cell.* 75:597–601.

Ohishi, J., M. Iwasaki, and G. Sakagushi. 1980. Purification and characterization of two components of *C. botulinum* C2 toxin. *Infect. Immun.* 30:668–673.

Orci, L., D. J. Palmer, M. Amherdt, and J. E. Rothman. 1993. Coated vesicle assembly in the Golgi requires only coatomer and ARF proteins from the cytosol. *Nature (Lond.).* 364:732–734.

Palmer, D. J., J. B. Helms, C. J. M. Beckers, L. Orci, and J. E. Rothman. 1993. Binding of coatomer to Golgi membranes requires ADP-ribosylation factor. *J. Biol. Chem.* 268:12083–12089.

Paterson, H. F., A. J. Self, M. D. Garrett, I. Just, K. Aktories, and A. Hall. 1990. Microinjection of recombinant $p21^{rho}$ induces rapid changes in cell morphology. *J. Cell Biol.* 111:1001–1007.

Pfeffer, S. R. 1992. GTP-binding proteins in intracellular transport. *Trends Cell Biol.* 2:41–46.

Ridley, A. J., H. F. Paterson, C. L. Johnston, D. Diekmann, and A. Hall. 1992.

The small GTP-binding protein rac regulates growth factor-induced membrane ruffling. *Cell.* 70:401–410.

Ridley, A. J., and A. Hall. 1992. The small GTP-binding protein rho regulates the assembly of focal adhesions and actin stress fibers in response to growth factors. *Cell.* 70:389–399.

Ridley, A. J., and A. Hall. 1994. Signal transduction pathways regulating Rho-mediated stress fibre formation: requirement for a tyrosine kinase. *EMBO J.* 13:2600–2610.

Rothman, J. E., and L. Orci. 1992. Molecular dissection of the secretory pathway. *Nature (Lond.).* 355:409–415.

Salminen, A., and P. J. Novick. 1987. A *ras*-like protein is required for a post-Golgi event in yeast secretion. *Cell.* 49:527–538.

Sandvig, K., and B. van Deurs. 1994. Endocytosis without clathrin. *Trends Cell Biol.* 4:275–277.

Schmalzing, G., S. Kröner, and H. Passow. 1989. Evidence for intracellular sodium pumps in permeabilized *Xenopus laevis* oocytes. *Biochem. J.* 260:395–399.

Schmalzing, G., P. Eckard, S. Kröner, and H. Passow. 1990. Downregulation of surface sodium pumps by endocytosis during meiotic maturation of *Xenopus laevis* oocytes. *Am. J. Physiol.* 258:C179–184.

Schmalzing, G., S. Gloor, H. Omay, S. Kröner, H. Appelhans, and W. Schwarz. 1991*a*. Up-regulation of sodium pump activity in *Xenopus laevis* oocytes by expression of heterologous β1 subunits of the sodium pump. *Biochem. J.* 279:329–336.

Schmalzing, G., K. Mädefessel, W. Haase, and K. Geering. 1991*b*. Immunocytochemical evidence for protein kinase C-induced internalization of sodium pumps in *Xenopus laevis* oocytes. *In* The Sodium Pump: Recent Developments. P. De Weer and J. H. Kaplan, editors. Rockefeller University Press, NY. 465–470.

Schmalzing, G., S. Kröner, M. Schachner, and S. Gloor. 1992. The adhesion molecule on glia (AMOG/β2) and α1 subunits assemble to functional sodium pumps in *Xenopus* oocytes. *J. Biol. Chem.* 267:20212–20216.

Schmalzing, G. 1994. Endo-exocytotic sorting of Na^+/K^+-pumps in developing oocytes and embryos of *Xenopus laevis*. *In* The Sodium Pump. E. Bamberg and W. Schoner, editors. Steinkopff, Darmstadt; Springer, New York. 147–158.

Schmitt, H. D., M. Puzicha, and D. Gallwitz. 1988. Study of a temperature-sensitive mutant of the *ras*-related *YPT1* gene product in yeast suggests a role in the regulation of intracellular calcium. *Cell.* 53:635–647.

Segev, N., J. Mulholland, and D. Botstein. 1988. The yeast GTP-binding YPT1 protein and a mammalian counterpart are associated with the secretory machinery. *Cell.* 52:915–924.

Sekine, A., M. Fujiwara, and S. Narumiya. 1989. Asparagine residue in the *rho* gene product is the modification site for botulinum ADP-ribosyltransferase. *J. Biol. Chem.* 264:8602–8605.

Spurr, A. R. 1969. A low-viscosity epoxy resin embedding medium for electron microscopy. *J. Ultrastruct. Res.* 26:31–43.

Stamnes, M. A., and J. E. Rothman. 1993. The binding of AP-1 clathrin adaptor particles to Golgi membranes requires ADP-ribosylation factor, a small GTP-binding protein. *Cell.* 73:999–1005.

Takaishi, K., A. Kikuchi, S. Kuroda, K. Kotani, T. Sasaki, and Y. Takai. 1993. Involvement of *rho* p21 and its inhibitory GDP/GTP exchange protein (*rho* GDI) in cell motility. *Mol. Cell. Biol.* 13:72–79.

Tominaga, T., K. Sugie, M. Hirata, N. Morii, J. Fukata, A. Uchida, H. Imura, and S. Narumiya. 1993. Inhibition of PMA-induced, LFA-1-dependent lymphocyte aggregation by ADP ribosylation of the small molecular weight GTP binding protein, *rho*. *J. Cell Biol.* 120:1529–1537.

Touchot, N., P. Chardin, and A. Tavitian. 1987. Four additional members of the *ras* gene superfamily isolated by an oligonucleotide strategy: molecular cloning of YPT-related cDNAs from a rat brain library. *Proc. Nat. Acad. Sci. USA.* 84:8210–8214.

Trowbridge, I. S., J. F. Collawn, and C. R. Hopkins. 1993. Signal-dependent membrane protein trafficking in the endocytic pathway. *Annu. Rev. Cell Biol.* 9:129–161.

van der Sluijs, P., M. Hull, P. Webster, P. Mâle, B. Goud, and I. Mellman. 1992. The small GTP-binding protein rab4 controls an early sorting event on the endocytic pathway. *Cell.* 70:729–740.

Vasilets, L. A., G. Schmalzing, K. Mädefessel, W. Haase, and W. Schwarz. 1990. Activation of protein kinase C by phorbol ester induces downregulation of the Na^+/K^+-ATPase in oocytes of *Xenopus laevis*. *J. Membr. Biol.* 118:131–142.

Vasilets, L. A., T. Ohta, S. Noguchi, M. Kawamura, and W. Schwarz. 1993. Voltage-dependent inhibition of the sodium pump by external sodium: species-differences and possible role of the N-terminus of the α-subunit. *Eur. Biophys. J.* 21:433–443.

Wiegers, W., I. Just, H. Müller, A. Hellwig, P. Traub, and K. Aktories. 1991. Alteration of the cytoskeleton of mammalian cells cultured in vitro by *Clostridium botulinum* C2 toxin and C3 ADP-ribosyltransferase. *Eur. J. Cell Biol.* 54:237–245.

Yisraeli, J. K., and D. A. Melton. 1989. Synthesis of long, capped transcripts *in vitro* by SP6 and T7 RNA polymerases. *Methods Enzymol.* 180:42–50.